On the Performance of Ad Hoc Networks with Multiuser Detection, Rate Control and Hybrid ARQ

Marco Levorato and Michele Zorzi

Dept. of Information Engineering, University of Padova, via Gradenigo 6/B, 35131 Padova, Italy. E-mail: {levorato,zorzi}@dei.unipd.it.

Abstract

In this paper, we present a novel analytical framework for the study of a multiple access scheme for an ad hoc CDMA network with HARQ error control and MF-LSIC receivers. Unlike most of the literature on Multi-User Detection (MUD), we directly address networking issues. In particular, we develop an approach based on renewal and semi-Markov processes, that accurately accounts for the statistical dependencies between interference, coding rate, and performance in a multiple access system. We show that our approximate approach can accurately predict throughput and failure rate values, and present results for a specific system, providing useful insight on issues related to the use of HARQ error control and MUD receivers in CDMA ad hoc networks.

I. Introduction

Nowadays wireless ad hoc networks suffer severe performance degradation due to the poor reuse of the channel resource achieved by carrier sense multiple access with collision avoidance (CSMA/CA) protocols. In fact, in order to protect ongoing communications from interference, the neighbors of both source and destination are denied access to the channel for the whole duration of the transmission. Moreover, hidden terminal and exposed terminal problems further increase the throughput loss. Thus, the throughput actually achieved is the result of a tradeoff between failure rate and spatial reuse, which is far from being optimized in CSMA/CA systems.

The use of multiuser detection (MUD) receivers appears to be a promising technology for future networking, and considerable research effort has recently gone into designing and analyzing efficient and effective MUD receiver structures. In particular, we focus on single antenna direct-sequence code-division multiple-access (DS-CDMA) systems, where multiple users transmit over the channel using distinct signature waveforms. Besides the well–known conventional DS-CDMA matched filter (MF) receiver, several other structures have been proposed. The DS-CDMA MF linear successive interference cancellation (MF-LSIC) receiver [1] sequentially decodes and cancels the signals in descending power order using an MF receiver at each stage. The MMSE-LSIC receiver [2], [3] is similar to the MF-LSIC receiver, except that an MMSE receiver is employed for signal detection. An improved version of the MMSE-LSIC receiver has been proposed in [4]. A powerful and attractive receiver structure is the joint iterative decoder [5]–[7], where the receiver performs an iterative algorithm exchanging soft information between the receiver components. A comparison of several DS-CDMA receivers is provided in [8].

The good performance of LSIC receivers and their relatively low complexity compared with maximum likelihood (ML) optimum receivers have generated a considerable effort in characterizing their behavior. In this paper, we focus our attention on DS-CDMA LSIC receivers, taking the results contained in [9] as the starting point of our analysis.

Despite the great amount of work done on the MUD PHY layer, limited work on CDMA MUD network analysis and design has been done so far. In [10], Tse *et al.* define the effective interference and bandwidth for large systems with power control and random spreading sequences, and investigate

the capacity achieved employing several multiuser receivers for a single–cell cellular network. Nie *et al.* [11] analyze the capacity of multi–cell cellular environments through reverse–link analysis. Ulukus *et al.* in [12] propose an iterative algorithm for optimizing the capacity of cellular networks with DS–CDMA MF systems.

Moreover, very little work exists regarding the issues arising when using CDMA MUD systems in ad hoc networks. In [13], [14], the authors analyze a single-code DS-CDMA MF system based on the ALOHA access protocol. In [15] a system with iterative multiuser detection and DS-CDMA MF detection for decoding the packet and the preamble, and with an ALOHA based access scheme is presented. [16] analyzes the performance of a DS/CDMA MF slotted system with ARQ and random arrivals through a processor-sharing system model.

One of the distinctive features of the present paper is to provide an in depth discussion of the performance of MUD ad hoc networks. In particular we focus on the interaction between the error control algorithm and the interference in a rate controlled network where multiple communications are allowed to take place at the same time.

The desire to fully exploit MUD in ad hoc networks opens several design challenges, that also involve MAC and higher communication layers. In ad hoc networks with standard receivers, MAC protocols basically try to avoid simultaneous transmissions in the same neighborhood, as they are likely to achieve a failure due to mutual interference. In this framework rate, power and error control are generally intended to counteract channel gain conditions and access scheme failures. In a scenario where nodes are equipped with MUD receivers, collision avoidance protocols may severely limit performance. In fact, thanks to the interference rejection capability of MUD receivers, the effect of the SINR loss due to interference is generally reduced with respect to standard receivers. Thus, the overall network throughput is likely to achieve its maximum if multiple communications take place at the same time.

The concurrency of communications increases the unpredictability of the channel status, especially in networks with distributed control, where nodes are not likely to know other nodes' decisions.

Moreover, nodes are generally not aware of the channel conditions of other receivers[1]. Thus, a node that wants to access the channel does not have an a priori knowledge of the effect of its transmission on the other ongoing communications.

It is important to observe that channel predictability in terms of interference is heavily dependent on the control algorithms, and in particular on the error control policy used. For instance, a retransmission based error control scheme may result in a higher interference unpredictability due to the higher overall birth rate. Conversely, an algorithm that relies on strong encoding (such as a pure FEC scheme) increases the interference correlation because of the longer transmission time and the generally lower failure probability. Thus, the efficiency of the control schemes plays a key role in this scenario, since it not only directly influences the amount of interference in the network, but also the interference statistics. In particular the choice of the error control scheme in simultaneous access networks is critical since it realizes the tradeoff between communications reliability and per packet resource expense, especially under variable conditions. Hybrid automatic retransmission request (HARQ) schemes have proven to be more efficient than classic ARQ or pure FEC schemes under highly variable conditions. While in ARQ schemes packets that failed to be received are simply retransmitted over the channel, typically after a random backoff interval, Type I and Type II Hybrid ARQ schemes exploit coding in order to increase efficiency and throughput. In Type I HARQ schemes, packets are encoded before being sent over the channel in order to increase the reliability of the transmission. Upon a decoding failure, the source sends again the same frame, much as in ARQ schemes. Type II schemes, instead, transmit incremental redundancy as instantaneously needed. A low-rate mother code is used to generate a large amount of redundancy, which is then used one piece at a time, so that further redundancy (which corresponds to a lower code rate) is used only when actually needed. The main advantage of Type II HARQ with respect to ARQ and Type I HARQ is this capability to dynamically adapt the coding rate to the instantaneous channel conditions. The investigation and the design of effective HARQ protocols and rate–compatible codes for various scenarios and applications have recently been attracting significant interest in the technical literature [17]–[23].

[1]To provide full knowledge of all nodes status generally requires a too heavy signaling overhead. However, nodes can collect information from other communications signaling. For instance, a node can estimate the channel toward currently receiving network nodes through feedback messages. The decoding of these messages allows nodes to acquire other communications status to improve the effectiveness of distributed load control

From the above discussion, it is clear that ad hoc networks, MUD receivers, multiple access and HARQ are important areas of research. In this paper, we bring them together into a comprehensive study, and provide a discussion of how the error control system interacts with the interference distribution, and thus with the overall performance, in a DS-CDMA ad hoc network with MF-LSIC at the receiver, HARQ and multiple simultaneous transmissions. More specifically, in this paper we make the following original contributions: (i) we explicitly include the use of ARQ and HARQ schemes in the considered system, and study their interactions with MUD and multiple access; (ii) we address the issue of multiple access MUD performance in an ad hoc networking setting, and develop a novel analytical framework to model the system and evaluate the metrics of interest – this framework, based on the theory of renewal and semi-Markov processes, accurately models interference relationships, and explicitly accounts for transmission overlaps and for the different statistics of the interference duration and rate of transmission due to biased sampling that results from random observations in time; (iii) as a concrete example of application, we provide specific results for a detailed system, namely a multiple access scheme in an ad hoc network based on DS-CDMA and HARQ, with MF-LSIC at the receiver. However, we remark that our analytical framework has a much wider applicability, and can be used in general to study multiple access systems with MUD and HARQ.

II. System Description

We investigate the performance of an ad hoc network where source nodes have to deliver packets of fixed length L [bits] to their intended destinations. Nodes transmit with fixed power P_{t}, and the transmission rate is set according to the perceived post-processing SINR. We assume that sources use a binary capacity–achieving code, so that for sufficiently long codewords the error probability vanishes when the link capacity is higher than the transmission rate. The encoded bits are then modulated and transmitted.

The protocol divides data transmission into three phases. In the first phase source and destination perform the handshake, in which the source transmits a request packet and the destination responds with a confirmation packet[2]. If the handshake succeeds, the source performs the second phase transmitting the data packet. In the third phase the destination sends out a feedback packet, in

[2]Unlike in 802.11, this exchange is performed without resorting to carrier sensing, thanks to the MUD capabilities of the receiver.

which it reports whether or not the packet has been successfully decoded. Our scheme provides that the confirmation packet contains the post–processing SINR associated with the source signal, as perceived by the destination during the reception of the request packet. Based on this value, the source sets the transmission rate of the data packet following one of the rate/error control policies listed below. Since handshake and feedback packets are generally much shorter than data packets, in the following discussion we idealize these parts of the communication. In particular, as a first step in this analysis, we assume that the handshake packet exchange and the destination feedback are error–free, that these phases are performed transmitting at fixed rate and that they do not interfere with ongoing communications[3]. We set the handshake duration to T_{H}.

Since interference and channel gain conditions may vary during a communication due to fading and to the start and end of other transmissions, we have that the post–processing SINR $S(t)$ of the intended signal is a function of the time index t, where $t = 0$ is the start of the transmission. To characterize the outage event we adopt the integral form

$$\xi_T = \left\{ W \int_{T_{\mathrm{H}}}^{T_{\mathrm{H}}+T} \log_2 \left(1 + S(t)\right) \mathrm{d}t < L \right\}, \tag{1}$$

where W is the bandwidth, $T = L/R$ is the transmission duration and R $[\mathrm{bits/s}]$ is the transmission rate. The integral form is the limit of the sum of the capacity for parallels channels, where fragments of the same codeword are sent over different channels, and is useful to keep the framework general. However, some scenarios, such as block fading and time slotted communications, allow the classic sum–rate capacity formulation, where the integral is replaced by the sum of the capacities of time intervals in which the SINR is assumed constant.

Note that $S(0)$ corresponds to the SINR at the start of a handshake transmission, while $S(T_{\mathrm{H}})$ corresponds to the SINR at the beginning of the data packet transmission. In the following we describe the considered transmission protocols.

A. Rate and Error Control

As mentioned before, communication is set up with a handshake phase meant to check destination availability and select the transmission rate. The computation of the minimum transmission time

[3]This assumption is satisfied for instance using a robust modulation/coding scheme or a dedicated control channel for the exchange of the handshake packets.

T^* is based on the instantaneous channel conditions during the handshake. This corresponds to the maximum rate that allows correct decoding if the channel remains constant during the transmission. We define this value for the rate as $R^* = W \log_2 (1 + S(0))$. For all the described policies the maximum allowed transmission duration is equal to $T_{\max}$.

• *ARQ Protocol*: In this protocol the source sets the value of the transmission rate to $R = R^*$. If a reception failure occurs, the source performs a further delivery attempt, including the handshake, after a random backoff interval. The process continues until the destination successfully decodes the packet or the maximum allowed number of transmissions F is reached. If a failure occurs at the F-th transmission attempt, the source dismisses the packet, leaving its recovery to the higher protocol layers. We denote as communication the whole data packet delivery attempt, including the possible retransmissions.

• *type I HARQ Protocol*: In type I HARQ schemes the packet is encoded with a rate $\rho \leq 1$ code. Assuming a capacity–achieving code this simply results in a lower transmission rate. Therefore we set the rate to $R = \rho R^*$, and consequently the duration is $T = T^*/\rho$. Thus, the smaller the value of ρ, the larger the redundancy sent. If the destination fails to decode the packet, the source starts the retransmission process as in the ARQ protocol before discarding the packet.

• *type II HARQ Protocol*: In this protocol the packet is encoded with a low rate code obtaining a long codeword and each delivery attempt is divided into two phases. In the first phase the source transmits a portion of the codeword, that corresponds to a transmission rate $R' = \eta' R^*$ for a time equal to $T' = T^*/\eta'$, then the destination sends out the feedback packet. If a decoding failure occurs, the feedback packet contains the value $S(T' + T_{\mathrm{H}})$, and the source starts the second phase. The transmission rate for the second phase is $R'' = \eta'' W \log_2 (1 + S(T' + T_{\mathrm{H}}))$, and therefore the second phase duration is

$$T'' = \frac{L - W \int_0^{T'} \log_2 (1 + S(t)) dt}{R''}. \tag{2}$$

η' and η'' are constrained only to be positive real numbers. The total data transmission time is $T = T' + T''$.

This protocol allows a greater adaptation to channel variations than type I HARQ, since the rate is computed again taking into account the perceived SINR during the first phase. While $\eta' \leq 1$ is

a conservative choice, for $\eta' > 1$ the protocol is more aggressive, because the source selects a rate higher than the estimated capacity to shorten the transmission in case of good channel, relying on the second phase if the channel does not support the chosen rate.

As for the previous protocols, if the destination reports a failure at the end of the transmission the source performs a further independent delivery attempt, until a success is achieved or the maximum number of allowed transmissions F is reached.

III. System Analysis

In this Section we derive the interference and SINR distributions needed for the performance analysis of the following Sections. The node density is equal to μ $[\mathrm{nodes/m^2}]$ and packet arrivals are modeled as a Poisson process of intensity λ $[\mathrm{pkts/s}]$ per node. We assume that the maximum destination distance is set to $R_{\max}$[4], and that the position of the destination node for a packet is uniformly distributed in the circular area of radius $R_{\max}$.

To model the interference, we consider a circular area A of radius $R_{\max}$, centered on the destination node. Therefore, given the node spatial distribution and the per node packet arrival rate λ, the overall arrival process of all transmitting sources is a Poisson process of intensity $\nu = \mu\lambda\pi R_{\max}^2$, and their positions are uniformly distributed in A. Fig. 1 depicts an example of source-destination pair placements, where the source and the destination of the communication we are focusing on, and the interfering sources and destinations are denoted with $\mathbf{S}$, $\mathbf{D}$, $\mathbf{I_k^S}$ and $\mathbf{I_k^D}$, respectively. The probability that the intended signal source $\mathbf{S}$ is at distance $\delta \leq \delta^*$ from node $\mathbf{D}$ is

$$\mathcal{F}_\delta(\delta^*) = \mathcal{P}\left\{\mathcal{D}(\mathbf{S},\mathbf{D}) \leq \delta^*\right\} = \frac{(\delta^*)^2}{R_{\max}^2}, \tag{3}$$

with associated pdf $f_\delta(\delta^*) = \mathrm{d}\mathcal{F}(\delta^*)/\mathrm{d}\delta^* = 2\delta^*/R_{\max}^2$, where $\mathcal{D}(N_1, N_2)$ is the distance between nodes N_1 and N_2. Observe that in this framework the distance of the interfering transmitters $\mathbf{I_k^S}$ with respect to $\mathbf{D}$, and the distance between $\mathbf{I}_k^S$ and $\mathbf{I}_k^D$ are also distributed according to $F_\delta(\delta^*)$, i.e.,

$$\mathcal{P}\left\{\mathcal{D}(\mathbf{S},\mathbf{D}) \leq \delta^*\right\} = \mathcal{P}\left\{\mathcal{D}(\mathbf{D},\mathbf{I}_k^S) \leq \delta^*\right\} = \mathcal{P}\left\{\mathcal{D}(\mathbf{I}_k^S,\mathbf{I}_k^D) \leq \delta^*\right\} = \mathcal{F}_\delta\left(\delta^*\right). \tag{4}$$

[4]Nodes farther away are neglected as a source of interference and are not chosen as destinations for packets generated by the nodes

A. Distribution of the Number of Interferers

In this Section we derive the distribution of the number of interfering transmissions during the communication between $\mathbf{S}$ and $\mathbf{D}$.

We denote with $\mathcal{G}_\delta(\tau)$ the cdf of the time duration of a generic communication where the source node and the destination node are placed at distance δ. In particular, given the distance δ, the probability that the communication duration T, without considering the hanshake, is less than or equal to τ is $\mathcal{G}_\delta(\tau) = \mathcal{P}\{T \leq \tau \mid \delta\}$. Moreover, we define $\Psi_\delta = \int_0^{T_{\max}} \mathcal{P}\{\xi_\tau \mid \delta\} \, \mathrm{d}\mathcal{G}_\delta(\tau)$ as the average failure probability of a single transmission between nodes N_1 and N_2, where $\mathcal{D}(N_1, N_2) = \delta$. Thus, the average number of transmissions for the communication between nodes N_1 and N_2 is

$$\Delta_\delta = \sum_{h=1}^{F-1} h \Psi_\delta^{h-1}(1 - \Psi_\delta) + F\Psi_\delta^{F-1} = \frac{1 - \Psi_\delta^F}{1 - \Psi_\delta}. \tag{5}$$

In the following we assume that $\mathcal{G}_\delta(\tau)$ and Ψ_δ are known. Section V describes the recursive process through which these distributions are computed.

It is important to observe that the retransmission process provided by the HARQ/ARQ protocols biases the distribution of the distances between the various sources and their intended destinations, while the distribution of the distance between the interfering transmitters and the other communication destinations remains $\mathcal{F}_\delta(\delta^*)$. This is one of the key points of our investigation, because any changes in the source-destination distribution may heavily affect the system interference distribution, due to the dependence between the destination distance and the communication length. In fact, although the rate control has the aim of ensuring equal reliability to in range communications, transmissions to distant destinations may achieve worse performance due to the longer duration on average, that may reduce interference correlation, and the worse channel statistics. Moreover, the minimum rate constraint may also increase the failure probability of these communications.

Therefore transmissions to distant destinations generally suffer higher failure probability with respect to those directed to closer destinations, and the former generally incur a higher number of retransmissions. Moreover, as stated before, the higher the distance of the destination, the higher the probability that the perceived SINR is low, and consequently the source transmission has a longer duration due to the lower transmission rate. Therefore, due to the retransmission process, the number of interfering nodes and the probability that an interfering node is active at a given time t given that

it was active at time $t - t^*$ are generally increased with respect to the single transmission case and the statistics of the transmission duration is biased.

Consider now a single source node that selects packet destinations with distance distribution $\mathcal{F}_\delta(\delta^*)$ and then transmits according to the communication protocol described in Section II. When a packet is either delivered or discarded, the source selects another destination for the next packet and so on. We sample the process at instants t_k, $k = 1, \ldots, \infty$, corresponding to the beginning of a transmission (or retransmission), and we call δ_{t_k} the distance between the source and the intended destination of the transmission starting at t_k. We are interested in the steady–state distribution of δ_{t_k}, i.e., $\lim_{k\to\infty} \mathcal{P}\left\{\delta_{t_k} \leq \delta^*\right\}$. This process can be modeled with a Semi–Markov process whose embedded chain is shown in Fig 2, where state i, $i = 1, 2, \ldots, I$, represents a complete communication, that may include several transmissions, to a destination at distance in $((i-1)\Theta, i\Theta]$, with $I\Theta = R_{\text{max}}$. Note that the transition probability between a state i and a state j does not depend on i, due to the independence of the destinations selection[5], and is equal to

$$p_{\{i,j\}} = \int_{(j-1)\Theta}^{j\Theta} f_\delta(\delta^*)\mathrm{d}\delta^* = \mathcal{F}_\delta(j\Theta) - \mathcal{F}_\delta((j-1)\Theta). \tag{6}$$

We also define the average failure probability of a single transmission given state i as

$$\Psi_i = \mathcal{P}\left\{\text{error} \mid i\right\} = \int_{(i-1)\Theta}^{(i)\Theta} \Psi_\delta \mathrm{d}\delta. \tag{7}$$

The average time, expressed in transmissions, that the Semi–Markov process spends in state i[6] is equal to the average number of transmissions that the source performs when communicating with a destination at distance in $((i-1)\Theta_D, i\Theta_D]$, i.e.,

$$S_i = \frac{1 - \Psi_i^F}{1 - \Psi_i}. \tag{8}$$

Observe that all rows of the transition matrix are equal to each other, and thus the steady–state probability of state i is $\pi_i = p_{\{.,i\}}$. Therefore, the average fraction of time, in transmissions, that the Semi–Markov process spends in states $i \leq i^*$ is [24]

$$B_{i^*} = \frac{\sum_{i=1}^{i^*} \pi_i S_i}{\sum_{i=1}^{I} \pi_i S_i}. \tag{9}$$

[5]Note that the semi-Markov process model is not strictly necessary, due to independence of destination selections. However, it makes the discussion more intuitive and keeps the following derivation more general.

[6]The described chain can be seen as the reduced version of the chain where each state i is composed of F states i_u, each representing a single transmission. The process moves from i_u to i_{u+1}, $u < F$, with probability Ψ_i, while with probability $(1 - \Psi_i)p_{\{i,j\}}$ moves toward one of the states i_j, $j = 1, \ldots, I$. From states i_u it moves to j_1 with probability $p_{\{i,j\}}$. The average time spent in states $i_1, \ldots, i_F$ is s_i.

Let $\Theta \to 0$ with $\Theta i^* = \delta^*$ and $\Theta I = R_{\max}$. Then,

$$\lim_{\Theta\to 0} \pi_{i^*} = \lim_{\Theta\to 0} \mathcal{F}_\delta((i^*+1)\Theta) - \mathcal{F}_\delta(i^*\Theta) = \mathcal{F}_\delta(\delta^*)\mathrm{d}\delta^* \qquad \lim_{\Theta\to 0} \Psi_{i^*} = \Psi_{\delta^*}, \tag{10}$$

and therefore, we get

$$\lim_{\Theta\to 0} B_i = \lim_{\Theta\to 0} \frac{\sum_{i=1}^{i^*} \pi_i S_i}{\sum_{i=1}^{I} \pi_i S_i} = \frac{\int_0^{\delta^*} \Delta_\delta f_\delta(\delta)\mathrm{d}\delta}{\int_0^{R_{\max}} \Delta_\delta f_\delta(\delta)\mathrm{d}\delta} = \mathcal{F}'_\delta(\delta^*). \tag{11}$$

$\mathcal{F}'_\delta(\delta^*)$ represents the distribution of the distance of the destination of a new transmission. A similar argument could be applied to derive the distance distribution of the destination of an ongoing communication, denoted with $\mathcal{F}''_\delta(\delta^*)$. The average duration of a transmission to a destination at distance δ is

$$\Omega_\delta = \int_0^{T_{\max}} (1 - \mathcal{G}_\delta(\tau))\,\mathrm{d}\tau. \tag{12}$$

The process required for obtaining $\mathcal{F}''_\delta(\delta^*)$ is similar to what described for the new communications distribution, except that in this case we continuosly sample the process, so that we obtain a continuous–time Semi–Markov process. Thus, the average time, in seconds, the Semi–Markov process spends in state i is $V_i = S_i\Omega_i$, where

$$\Omega_i = \int_{(i-1)\Theta}^{i\theta} \Omega_\delta \mathrm{d}\delta. \tag{13}$$

Hence, with a derivation analogous to that of $\mathcal{F}'_\delta(\delta^*)$ we get

$$\mathcal{F}''_\delta(\delta^*) = \frac{\int_0^{\delta^*} \Delta_\delta \Omega_\delta f_\delta(\delta)\mathrm{d}\delta}{\int_0^{R_{\max}} \Delta_\delta \Omega_\delta f_\delta(\delta)\mathrm{d}\delta}. \tag{14}$$

We also define $f'_\delta(\delta^*) = \mathrm{d}\mathcal{F}'_\delta(\delta^*)/\mathrm{d}\delta^*$, $f''_\delta(\delta^*) = \mathrm{d}\mathcal{F}''_\delta(\delta^*)/\mathrm{d}\delta^*$.

We remark that $\mathcal{F}_\delta(\delta^*)$ represents the a priori distribution of the distance of nodes selected as destination for the packets, while $\mathcal{F}'_\delta(\delta^*)$ represents the distribution of the distance between the source and the destination of a new transmission, due to the dependence between the distance and the attempt rate (longer links need more transmission attempts and are therefore more likely to occur). $\mathcal{F}''_\delta(\delta^*)$ is the distribution of the distance of an ongoing transmission, resulting from the dependence between the destination distance and the attempt rate and length (when sampling in time, it is more likely to find ongoing transmissions with longer distance, i.e., lower rate and longer duration).

We now characterize the process $Z(t)$, where $Z(t) = z$ if at time $t \geq 0$ the communication from $\mathbf{S}$ to $\mathbf{D}$ has z interfering nodes and $t = 0$ corresponds to the start of the handshake.

We denote with $R(t^*)$ the process representing the number of already active communications at time $t=0$ that are still alive at time $t=t^*$. Ongoing communications have source–destination distance distribution $\mathcal{F}''_\delta(\delta^*)$, so that their average duration distribution and mean are

$$\mathcal{G}''(\tau)=\int_0^{R_{\max}}\mathcal{G}_\delta(\tau)f''_\delta(\delta^*)\mathrm{d}\delta^* \qquad\qquad \Omega''=\int_0^{T_{\max}}[1-\mathcal{G}''(\tau)]\,\mathrm{d}\tau. \tag{15}$$

Observing that $R(0)=Z(0)$, we model the number of ongoing interfering transmissions at time $t=0$ with the long run distribution of a Poisson arrival distribution with parameter ν and lifetime distribution $\mathcal{G}''(\tau)$, that is also Poisson with parameter $\nu\Omega''$ [24], i.e.,

$$\mathcal{P}\left\{R(0)=z_0\right\}=\frac{(\nu\Omega'')^{z_0}\,e^{-\nu\Omega''}}{z_0!},z_0=0,1,2,\ldots. \tag{16}$$

The probability that an active transmission at time $t=0$ is still active at time τ is the probability that its residual life ω is greater than or equal to τ^*, i.e.,

$$\mathcal{P}\left\{\omega\geq\tau^*\right\}=1-\frac{1}{\Omega''}\int_0^{\tau^*}[1-\mathcal{G}''(\tau)]\,\mathrm{d}\tau=1-\frac{\zeta''_{\tau^*}\tau^*}{\Omega''}, \tag{17}$$

where $\zeta''_{\tau^*}=\frac{1}{\tau^*}\int_0^{\tau^*}[1-\mathcal{G}''(\tau)]\mathrm{d}\tau$. Observing that $R(t^*)\leq R(0)$, with $t^*>0$, the probability that r of the $R(0)$ transmissions are still active at time t^* is then

$$\mathcal{P}\left\{R(t^*)=r\mid R(0)=z_0\right\}=\frac{z_0!}{r!(z_0-r)!}\left(1-\frac{\zeta''_{t^*}t^*}{\Omega''}\right)^r\left(\frac{\zeta''_{t^*}t^*}{\Omega''}\right)^{z_0-r}. \tag{18}$$

However, during this transmission time, new transmissions can also start and end, contributing to the total process $Z(t)$. We denote with $N(t^*)$ the number of new transmissions started in $(0,t^*)$, and with $M(t^*)$ the process counting the number of those transmissions that are still active at time $t=t^*$. $M(t^*)$ has Poisson distribution with mean $\nu\zeta'_{t^*}t^*=\nu\int_0^{t^*}[1-\mathcal{G}'(\tau)]\mathrm{d}\tau$ [24], i.e.,

$$\mathcal{P}\left\{M(t^*)=m\right\}=\frac{(\nu\zeta'_{t^*}t^*)^m\;e^{-\nu\zeta'_{t^*}t^*}}{m!},m=0,1,2,\ldots \tag{19}$$

where $\mathcal{G}'(\tau^*)=\int_0^{R_{\max}}\mathcal{G}_\delta(\tau^*)f'_\delta(\delta^*)\mathrm{d}\delta^*$. Therefore, the distribution of the total number of active transmissions at time τ^*, conditioned on the number of ongoing communications at time $t=0$, is

$$\begin{aligned}\mathcal{P}\{Z(\tau^*)=z\,|\,Z(0)=z_0\}&=\sum_{r=0}^{\min(z_0,z)}\mathcal{P}\{R(\tau^*)=r\mid Z(0)=z_0\}\,\mathcal{P}\{M(\tau^*)=z-r\}\\&=\sum_{r=0}^{\min(z,z_0)}\frac{z_0!}{r!(z_0-r)!}\left(1-\frac{\zeta''_{\tau^*}\tau^*}{\Omega''}\right)^r\left(\frac{\zeta''_{\tau^*}\tau^*}{\Omega''}\right)^{z_0-r}\frac{(\nu\zeta'_{\tau^*}\tau^*)^{(z-r)}e^{-\nu\zeta'_{\tau^*}\tau^*}}{(z-r)!}.\end{aligned} \tag{20}$$

Fig. 3 depicts a graphical representation of the described processes. It is important to observe that the proposed analysis considers the average transmission length distributions, and it is therefore approximated in the sense that the correlation between the number of actual interfering nodes and the length distribution is ignored. In fact, given for instance a high number of interfering transmissions, their length would tend to be generally greater than in the presence of a lower number of users, due to the generally low SINR that the destinations of these communications might perceive at the start of the handshake. Our results have shown that this approximation is accurate.

IV. PHY Layer and Performance Approximation

A. Receiver Model and Performance Approximation

In this Section we summarize the considered transmitter/receiver structure and the performance approximation derived in [9], which is used to model the output SINR throughout the paper. As stated in the Introduction, we focus our attention on the DS-CDMA MF and MF LSIC receivers. For the sake of simplicity, in our analysis we consider chip–synchronous transmissions, and we refer the reader to [25] for an in–depth discussion of the performance of asynchronous systems. Let $\gamma_1, \ldots, \gamma_K$ be the received powers of K users transmitting over an AWGN channel with binary phase–shift keying (BPSK) modulation. The input of the MF bank corresponding to the jth symbol is $\boldsymbol{c}^j = \sum_{i=1}^{K} \sqrt{\gamma_i} b_i^j \boldsymbol{s}_i + \boldsymbol{n}^j$, where $\boldsymbol{s}_i = [s_i^1, \ldots, s_i^N]$ is the vector of the N chips of the spreading sequence of the ith user and b_i^j is the jth bit of the ith user. $\boldsymbol{n}^j$ is the noise vector, whose N elements $n_1^j, \ldots, n_N^j$ are modeled as uncorrelated Gaussian random variables, with zero mean and variance σ^2. $\boldsymbol{c}^j$ contains the samples corresponding to the jth transmitted symbol. The BPSK symbols b_i^j, $\forall j, i$ are assumed to be independent and identically distributed. In the following we assume that s_i^h, $h = 1, \ldots, N$ are i.i.d. random variables with $s_i^h \in \{\pm 1/\sqrt{N}\}$, and $\mathcal{P}[s_i^h = 1/\sqrt{N}] = \mathcal{P}[s_i^h = -1/\sqrt{N}] = 1/2$.

The MF LSIC receiver sequentially decodes and removes from the overall received waveform the individual received signals in decreasing power order. At each of the K stages the receiver selects the user with the strongest received power, and performs the decoding. Assuming that the users are labeled in decreasing power order, so that $\gamma_i \geq \gamma_{i+1}$, $i = 1, \ldots, K-1$, the decision variable at the mth stage is $z_m^j = \boldsymbol{s}_i^T \tilde{\boldsymbol{e}}_m^j$, where $\tilde{\boldsymbol{e}}_m^j$ is the input of the mth stage of the MF LSIC receiver. The estimated symbol is then $\tilde{b}_m^j = sgn(z_m^j)$, where $sgn(\cdot)$ is the signum function. The estimated symbol

is then rescaled with the amplitude estimate of the MF bank, respread with $\boldsymbol{s}_m$ and subtracted from the received signal.

The mth stage input can be written as [26]

$$\tilde{\boldsymbol{e}}_m^j = \left(\mathbf{I} - \boldsymbol{s}_{m-1}\boldsymbol{s}_{m-1}^T\right)\tilde{\boldsymbol{e}}_{m-1}^j = \sum_{i=1}^{K}\sqrt{\gamma_i}b_i^j\mathbf{T}_m\boldsymbol{s}_i + \mathbf{T}_m\boldsymbol{n}, \tag{21}$$

where $\mathbf{I}$ is the identity matrix, and $\mathbf{T}_m = (\mathbf{I} - \boldsymbol{s}_{m-1}\boldsymbol{s}_{m-1}^T)\ldots(\mathbf{I} - \boldsymbol{s}_1\boldsymbol{s}_1^T)$. The decision variable at stage m is $\tilde{z}_m^j = \sqrt{\gamma_m}b_m^j\tilde{\psi}_{mm} + \sum_{i\neq m}\sqrt{\gamma_i}b_i^j\tilde{\psi}_{mi} + \tilde{n}_m$, where $\tilde{\psi}_{mi} = \boldsymbol{s}_m^T\mathbf{T}_m\boldsymbol{s}_i$ is the effective cross-correlation and $\tilde{n}_m = \boldsymbol{s}_m^T\mathbf{T}_m\boldsymbol{n}$ is the effective noise component.

In [9], approximations for the residual cancellation errors, the effective noise power and the interference due to still undecoded signals are derived. The approximated output SINR for the mth decoded user for the MF LSIC receiver, given the received powers $\gamma_1,\ldots,\gamma_K$, sorted in decreasing power order is

$$SINR^{\text{LSIC}} \approx \frac{\gamma_m\left(1-\frac{1}{N}\right)^{2(m-1)}}{\sum_{j<m}\gamma_j\left(\frac{j-1}{N^2}\right) + \sum_{j>m}\gamma_j\frac{1}{N}\left(1-\frac{1}{N}\right)^{m-1} + \sigma^2\left(1-\frac{1}{N}\right)^{m-1}}, \tag{22}$$

For the MF receiver, the output SINR is

$$SINR^{\text{MF}} \approx \frac{\gamma_m}{\sum_{j\neq m}\frac{\gamma_j}{N} + \sigma^2}. \tag{23}$$

B. SINR Distribution

To characterize the system performance we derive the average SINR distribution at time t, where $Z(t)=K$ is the number of transmitting users. We focus on the MF-LSIC case, since the MF case is straighforward. As in Section IV-A, we assume that the received powers, denoted with $\gamma_1,\ldots,\gamma_K$, are sorted in descending order.

We consider a Rayleigh block–fading channel model, so that at distance δ from a transmitter, the probability that the received power of the wanted signal at the destination, γ_s, is lower than γ^* is

$$\mathcal{J}_\delta(\gamma^*) = \mathcal{P}\left\{\gamma_s \leq \gamma^*\right\} = \int_0^{\gamma^*}\frac{1}{P_{\text{t}}\delta^{-\alpha}}e^{-\frac{x}{P_{\text{t}}\delta^{-\alpha}}}\mathrm{d}x = 1 - e^{\frac{\gamma^*}{P_{\text{t}}\delta^{-\alpha}}}, \tag{24}$$

where α is the path–loss exponent. The received interference power of a single transmitting node distribution is

$$\mathcal{J}(\gamma^*) = \int_0^{R_{\max}}\mathcal{J}_\delta(\gamma^*)f_\delta(\delta)\mathrm{d}\delta = 1 - \frac{2\left(\frac{\gamma^*}{P_{\text{t}}}\right)^{-\frac{2}{\alpha}}\left(\Gamma\left(\frac{2}{\alpha}\right) - \Gamma\left(\frac{2}{\alpha},\frac{\gamma^*R_{\max}^\alpha}{P_{\max}}\right)\right)}{\alpha R_{\max}^2}, \tag{25}$$

where $\Gamma(z) = \int_0^\infty t^{z-1}e^{-t}dt$ and $\Gamma(a,z) = \int_z^\infty t^{a-1}e^{-t}dt$ are the Gamma and the incomplete Gamma functions. We define the pdfs associated with $\mathcal{J}_\delta$ and $\mathcal{J}$ as $j_\delta(\gamma^*) = \mathrm{d}\mathcal{J}_\delta(\gamma^*)/\mathrm{d}\gamma^*$ and $j(\gamma^*) = \mathrm{d}\mathcal{J}(\gamma^*)/\mathrm{d}\gamma^*$, respectively.

The output SINR of the MF LSIC receiver is modeled with (22). Thus, considering a transmission from a source node $\mathbf{S}$ to a destination node $\mathbf{D}$, with $\mathcal{D}(\mathbf{S},\mathbf{D}) = \delta$, where the total number of interfering signals is K, the probability that the output SINR $S(t)$ is lower than or equal to S^*, given the received power ω_s^2 of the wanted signal, is

$$\begin{aligned}\mathcal{X}^K(S^*,\delta) &= \int_0^\infty \sum_{m^*=1}^{K+1} \mathcal{P}\left\{S \le S^* \mid m = m^*, \gamma_s\right\} \mathcal{P}\left\{m = m^* \mid \gamma_s\right\} j_\delta(\gamma_s)\mathrm{d}\gamma_s \\ &= \int_0^\infty \sum_{m^*=1}^{K+1} \mathcal{X}_{|\gamma_s}^{(K,m^*)}(S^*,\delta)\mathcal{P}\left\{m = m^* \mid \gamma_s\right\} j_\delta(\gamma_s)\mathrm{d}\gamma_s, \end{aligned} \tag{26}$$

where m is the decoding stage. From (22), we get

$$\mathcal{X}_{|\gamma_s}^{(K,m)}(\psi,\delta) = \int_{\gamma_s}^\infty j(\gamma_1)\left(\int_{\gamma_s}^{\gamma_1} j(\gamma_2)\left(\ldots\int_{\gamma_s}^{\gamma_{m-2}} j(\gamma_{m-1})Z_\psi^m(\boldsymbol{\gamma}_{m-1},\gamma_s)\mathrm{d}\gamma_{m-1}\ldots\right)\mathrm{d}\gamma_2\right)\mathrm{d}\gamma_1, \tag{27}$$

where $\boldsymbol{\gamma}_n$ denotes the vector $[\gamma_1,\ldots,\gamma_n]$. γ_s is equal to γ_m, since the wanted signal is decoded at stage m. $\mathcal{Z}_m^\psi(\boldsymbol{\gamma}_{m-1},\gamma_s)$ is defined as

$$\mathcal{Z}_m^\psi(\boldsymbol{\gamma}_{m-1},\gamma_s) = \int_0^{\min\left\{\gamma_s,\mathcal{S}_\psi^{m+1}(\boldsymbol{\gamma}_{m-1},\gamma_s)\right\}} j(\gamma_{m+1})\left(\ldots\int_0^{\min\left\{\gamma_{K-1},\mathcal{S}_\psi^{K}(\boldsymbol{\gamma}_{K-1},\gamma_s)\right\}} j(\gamma_K)\mathrm{d}\gamma_K\ldots\right)\mathrm{d}\gamma_{m+1},$$

where

$$\mathcal{S}_\psi^n(\boldsymbol{\gamma}_{n-1},\gamma_s) = \frac{\gamma_s}{\psi}\left(1-\frac{1}{N}\right)^2 - \frac{\sigma^2}{N} - \sum_{j<m}\gamma_j\frac{N\left(\frac{j-1}{N^2}\right)}{\left(1-\frac{1}{N}\right)^{m-1}} - \sum_{m<j<n}\gamma_j. \tag{28}$$

Now we evaluate the probability that the wanted signal is decoded at stage m^*, given the total number of transmitting nodes K and $\mathcal{D}(\mathbf{S},\mathbf{D}) = \delta$. Assuming that the received power of the wanted signal is γ_s, the probability that it is decoded at stage m^* is equal to

$$\mathcal{P}\left\{m = m^* \mid \gamma_s\right\} = \frac{(K-1)!}{(m^*-1)!(K-m^*)!}\left(1-\mathcal{J}(\gamma_s)\right)^{(m^*-1)}\left(\mathcal{J}(\gamma_s)\right)^{(K-m^*)}, \tag{29}$$

These integrals can be computed through numerical integration.

V. Recursive Performance Analysis

The distributions derived in the previous Section are required for assessing the network performance. To this end we set up an algorithm that recursively computes the system interference and failure distributions.

To keep the problem tractable we divide the time axis in slots of duration T_{S}. We assume that T_{S} is within the channel coherence time, so that fading coefficients remain constant during a slot. Moreover, we assume that users can start transmissions only at slots boundaries, and that the duration of each transmission is a multiple of T_{S}, which is reasonable if transmitters have only a finite set of rates. Note that in this setting the number of interfering nodes during each slot does not change. For the sake of simplicity, also the handshake duration is set to a multiple of the slot duration. The data packet transmission duration in slots is $N = \left\lceil \frac{L}{R_x T_{\mathrm{S}}} \right\rceil$, where R_x is the rate prescribed by the used protocol, and $\lceil \cdot \rceil$ is the ceiling operator.

The recursive algorithm takes as input the estimated distributions Ψ_δ and $\mathcal{G}_\delta(\tau)$, and the per node transmission arrival rate λ. Given Ψ_δ and $\mathcal{G}_\delta(\tau)$, the algorithm computes the distribution of the number of interfering transmissions at the beginning and during the transmission as described in Section III-A. Through Montecarlo trials the algorithm produces a further estimate of these distributions and collects the performance metrics described in V-A. In particular, for a fixed distance δ between the source and the destination, the number of slots N the transmission lasts is a function of the initial number of interferers. Thus, in the ARQ case the distribution of the length for the next iteration is given by

$$\begin{aligned}
&\tilde{\mathcal{G}}_\delta(N^* T_{\mathrm{S}}) = \mathcal{P}\left\{N \leq N^* \mid \mathcal{D}(\mathbf{S},\mathbf{D}) = \delta\right\} = \\
&= \sum_{z_0=1}^{\infty} \mathcal{P}\left\{ S(0) \geq 2^{\frac{L}{WN^*T_{\mathrm{S}}}} - 1 \mid \mathcal{D}(\mathbf{S},\mathbf{D}) = \delta, Z(0) = z_0 \right\} \mathcal{P}\left\{Z(0) = z_0\right\} \\
&= 1 - \sum_{z_0=1}^{\infty} \mathcal{X}^{z_0}(2^{\frac{L}{WN^*T_{\mathrm{S}}}} - 1, \delta) \frac{(\nu\Omega'')^{z_0}\, e^{-\nu\Omega''}}{z_0!},
\end{aligned} \tag{30}$$

where N is the number of slots where the source transmits. Note that the calculation of $\tilde{\mathcal{G}}_\delta(N^* T_{\mathrm{S}})$ is based on its estimate at the previous algorithm step. In the type I HARQ case the rate is scaled by a factor ρ. As to the failure probability, for the ARQ and type I HARQ this corresponds to the

event

$$\xi = \left\{ WT_{\mathrm{S}} \sum_{u=1}^{N} \log_2 \left(1 + S(uT_{\mathrm{S}})\right) < L \right\}. \tag{31}$$

$\tilde{\Psi}_\delta = \mathcal{P}\left\{\xi \mid \mathcal{D}(\mathbf{S},\mathbf{D}) = \delta\right\}$ is evaluated through the distribution of the number of users and the SINR distribution via Montecarlo integration. In the type II HARQ case, the distribution of the transmission length is

$$\begin{aligned} \tilde{\mathcal{G}}_\delta(N^* T_{\mathrm{S}}) &= \mathcal{P}\left\{N' \le N^* \mid \bar{\xi}', \mathcal{D}(\mathbf{S},\mathbf{D}) = \delta\right\} \mathcal{P}\left\{\bar{\xi}' \mid \mathcal{D}(\mathbf{S},\mathbf{D}) = \delta\right\} \\ &+ \mathcal{P}\left\{N' + N'' \le N^* \mid \xi', \mathcal{D}(\mathbf{S},\mathbf{D}) = \delta\right\} \mathcal{P}\left\{\xi' \mid \mathcal{D}(\mathbf{S},\mathbf{D}) = \delta\right\}, \end{aligned} \tag{32}$$

where N' and N'' are the lengths in slots of the first and second phase, and ξ' and $\bar{\xi}'$ represent the failure and success events in the first phase, respectively. As in the previous case, the various probabilities can be conditioned to the initial number of interferers and summed. Note that the distribution of the length of the second phase depends on the SINRs perceived in the first phase and the SINR of the last slot, i.e., $S(N'T_{\mathrm{S}})$.

Note also that the retransmission process changes not only the destination distance distribution of the interfering transmissions, but also the overall transmission arrival rate. The input arrival rate $\tilde{\lambda}$ for the next algorithm iteration is

$$\tilde{\lambda} = \lambda \int_0^{R_{\max}} \Delta_\delta f_\delta(\delta) \mathrm{d}\delta. \tag{33}$$

In the first iteration, the failure probability is set to zero. Observe that in this case $\mathcal{F}''_\delta(\delta^*) = \mathcal{F}'_\delta(\delta^*) = \mathcal{F}_\delta(\delta^*)$. The initial distribution of the source transmission length $\mathcal{G}_\delta(\tau)$ is evaluated for a number of interfering transmissions that is distributed according to a Poisson process of rate ν. With this distribution the evaluation of the initial failure probability is then performed.

A. Performance Metrics

Through the presented analysis and the distributions defined in Section III-A we obtain some metrics that are significant for characterizing the network performance.

The failure probability of the packet delivery, taking into account the various retransmissions, and conditioned to the destination distance $\delta = \delta^*$, is

$$\tilde{\Gamma}_{\delta^*} = 1 - \sum_{a=0}^{F-1} \left(\tilde{\Psi}_{\delta^*}\right)^a \left(1 - \tilde{\Psi}_{\delta^*}\right) = \left[\tilde{\Psi}_{\delta^*}\right]^F, \tag{34}$$

and the average number of transmissions is $\tilde{\Delta}_{\delta^*} = (1 - \tilde{\Psi}^F_{\delta^*})/(1 - \tilde{\Psi}_{\delta^*})$. We refer to their respective values averaged over the destination distance as $\tilde{\Gamma}$ and $\tilde{\Delta}$.

The overall throughput in [bps/Hz] achieved in the considered area is then

$$\mathcal{R} = \nu L \int_0^{R_{\max}} \frac{1 - \tilde{\Gamma}_\delta}{\Omega_\delta \tilde{\Delta}_\delta} f_\delta(\delta) \mathrm{d}\delta. \tag{35}$$

We also compute the average number of active interfering transmissions per slot as

$$\mathcal{U} = \sum_{z_0=0}^{\infty} \frac{\sum_{s=0}^{N^*} \sum_{k=0}^{\infty} k\mathcal{P}\left\{Z(s\Delta_T) = k \mid Z(0) = z_0\right\}}{N^*} \mathcal{P}\left\{N = N^* \mid Z(0) = z_0\right\} \mathcal{P}\left\{Z(0) = z_0\right\}.$$

VI. Results

In this section we present and discuss the results obtained with the system analysis developed in the previous sections. First, we compare the analytically obtained performance with the results of simulations that implement all the details of the HARQ process at both the source node and the interfering nodes. To avoid border effects, we consider a circular area of radius $QR_{\max}$, $Q \geq 1$, around the destination of which we collect the performance. This is useful to get a realistic transmission length distribution at the interfering nodes, that are in turn interfered by other transmissions. However, the interfering nodes at distance greater than $R_{\max}$ from the various destinations, including those of the interfering nodes, are ignored in the received SINR computation. Simulations are computationally much heavier than the analysis, due to the need to keep track of the status of all the ongoing communications (including those in backoff), and soon become infeasible as the number of communications increases, i.e., for high values of λ, ρ or F. In Table I, the values of the parameters used in both analysis and simulations are summarized.

Figs. 4, 5 and 6 give some examples of comparison between analysis and simulations. Many more cases have been run, and the match was observed to be fairly good in most cases. Fig. 4 compares the overall analytical throughput achieved in the considered area, computed as in (35), with the throughput obtained through simulations for the MF and MF LSIC cases with an ARQ scheme with two retransmissions as a function of the per node packet arrival rate λ. It is possible to observe that the analysis shows a good match with the simulations, especially in the LSIC case. The MF case is more sensitive to the approximation of the interfering transmission behavior with the averaged statistics. In fact, the MF receiver has a lower resilience to interference than the LSIC receiver and

then the correlation between the number and the duration of the interfering transmissions is greater. Fig. 5 shows the average duration of a transmission as a function of λ for the LSIC receiver with the type I HARQ scheme for $\rho = 1, 1/2, 1/3$. As expected, the lower the coding rate, the higher the transmission length. Note that the ratio of the average durations for $\rho = 1$ and $\rho = 1/2$ is not necessarily equal to 2. In fact, besides the coding gain, the duration depends on the perceived SINR and, thus, on the interference in the network. This results from the tradeoff between the single transmission failure probability, that is the retransmission probability in the case $F = 2$, and the single transmission length. Fig. 6 depicts the average delivery failure rate, including retransmissions, for the same cases considered in the previous plot, as a function of the coding rate ρ. The proposed analysis is slightly less accurate than for the throughput for high failure probabilities.

In the following, we present analytical results comparing the considered metrics for the various proposed schemes. In the following we set $\eta' = \eta'' = \eta$, leaving for future investigations the optimization of the performance that may come from a differentiation of the values for η' and η''. Figs. 7, 8 and 9 show respectively the average throughput, the number of interfering transmissions and the failure rate as a function of the node density μ achieved by the various proposed schemes for various values of F. As a first observation, for all the considered error control policies if the number of retransmissions allowed is increased the interference generated by the greater birth rate decreases the average transmission rate, and thus degrades the throughput. This effect is less noticeable in type I and II HARQ, where the higher probability that a transmission achieves a success reduces the retransmission probability and then the increase in birth rate. Moreover, for small network load a density increase results in a throughput improvement, while above a scheme–dependent threshold the throughput decreases as the density is further increased. This is due to the tradeoff between the gain due to a higher number of simultaneously deployed transmissions, and their average duration and failure probability.

Type II HARQ appears to be the best choice for the considered density range, as it achieves a good throughput preserving communication reliability even for a low number of allowed retransmissions. In fact, while type I HARQ relies on long transmissions to keep the failure probability low, and pure HARQ incurs too many failures, type II HARQ provides a good system balance. This is due to its

adaptability to highly varying channel conditions. However, as the density increases, the best choice in terms of throughput probably becomes early packet discarding and short transmission to reduce receivers' load. For very high density, as interference saturates the network, strong coding, and thus longer transmission, has a lower effect on throughput, so that it can be a good solution.

An interesting observation is that that while the failure probability generally increases as the density increases for the type I and II HARQ, the pure ARQ scheme decreases slightly before the entire network collapses. This is due to the longer duration of the transmissions as the network load increases, that provides an increased channel correlation in the ARQ schemes, that have a high failure probability and hence a high birth rate. This effect is negligible in schemes with lower retransmission probability and intrinsically higher duration, such as type I and II HARQ.

Fig. 10 depicts the throughput for different values of the density as a function of η for a single transmission. It is possible to observe that for average values of the node density, the throughput has a maximum for values close to $\eta = 1$, and the performance quickly degrades as the coding becomes stronger. For high densities, in which the interference load is higher, a greater load due to stronger encoding heavily affects the performance in terms of throughput, so that the maximum is achieved for more aggressive choices of η.

Fig. 11 shows the throughput vs. node density for type II HARQ and various values of η for $F = 1$ and 2. In this case it is important to observe that too aggressive or too conservative choices of the coding parameter can affect throughput. It is interesting to observe that while for $F = 1$ a too conservative choice of η, such as $\eta = 0.5$, heavily affects throughput, due to the average higher transmission duration that outweighs the improvement in terms of failure probability, for $F = 2$ and high values of the nodes density the scheme with $\eta = 0.5$ achieves the best performance. This is due to the reduced retransmission probability, that increases channel predictability. Moreover, this scheme accumulates the gain of two long transmissions, while for the other choices of η the receiver has a higher probability of discarding what was already received, relying on a further transmission.

We remark that the interaction between the interference, the transmission rate and the reliability in MUD networks is rather complex and involved. Therefore, the scheme the system relies on for packet delivery is critical for the achieved performance. Generally, too low an encoding rate results

in an increased transmission length, while too aggressive a transmission strategy incurs excessive additional retransmissions. Type II HARQ schemes, if accurately set, appear to be a good solution for both efficiently adapting the transmisson rate to the channel conditions and preserving the system reliability.

The initial results presented in this section highlight some interesting trade-offs that arise when combining HARQ, MUD, and multiple access in ad hoc networks. We believe that these behaviors, that are observed in this paper for the first time, deserve a deeper investigation, and can be expected to reveal interesting insights and to lead to strategies for the optimization of the network performance as a function of the lower layer design choices.

VII. Conclusions

In this paper, we have presented a novel analytical approach for the evaluation of multiple access in CDMA based ad hoc networks with HARQ error control and MF-LSIC receivers. We focused directly on networking issues, and provided a framework by which we can evaluate the performance of such systems via accurate interference stochastic modeling and a recursive technique. Comparison with simulation results shows that the method is accurate, and is able to correctly predict the behavior of important metrics, such as throughput and failure rates. Even though the proposed framework is rather general, we have presented specific results for a concrete system example, identifying interesting behaviors and providing useful insights on the use of HARQ error control and MUD receivers in ad hoc networks, which is still a largely unexplored area of research. Successive interference cancellation appears to be a promising technique for increasing the network capacity. However, for these kinds of receivers the dependence between the error control scheme, the transmitted power and the achieved performance is still an open issue, that we will consider as part of our future work.

References

[1] K. Lai and J. J. Shynk, "Performance evaluation of Generalized Linear SIC for DS/CDMA signals," *IEEE Trans. Signal Processing*, vol. 51, no. 6, pp. 1604–1614, June 2003.

[2] P. B. Rapajic and B. S. Vucetic, "Adaptive receiver structure for asynchronous CDMA systems," *IEEE J. Select. Areas Commun.*, vol. 12, pp. 685–697, May 1994.

[3] S. L. Miller, "An adaptive direct–sequence code–division multiple–access receiver for multiuser interference rejection," *IEEE Trans. Commun.*, vol. 43, pp. 1746–1755, Feb./Mar./Apr. 1995.

[4] Y. Cho and J. H. Lee, "Analysis of an adaptive SIC for near–far resistant DS-CDMA," *IEEE Trans. Commun.*, vol. 46, no. 11, pp. 1429–1432, Nov. 1998.

[5] C. Schlegel, Z. Shi, and M. Burnashev, "Optimal power/rate allocation and code selection for iterative joint detection of coded random CDMA," *IEEE Trans. on Inform. Theory, to appear*.

[6] P. Alexander, A. Grant, and M. Reed, "Iterative detection in code-division multiple-access with error control coding," *Eur. Trans. Telecommun.*, vol. 9, no. 5, pp. 419–426, Sept. 1998.

[7] P. D. Alexander, M. C. Reed, J. A. Asenstorfer, and C. Schlegel, "Iterative multiuser interference reduction: Turbo CDMA," *IEEE Trans. Commun.*, vol. 47, pp. 1008–1014, July 1999.
[8] P. H. Tan and L. K. Rasmussen, "Multiuser detection in CDMA – a comparison of relaxations, exact, and heuristic search methods," *IEEE Trans. Wireless Commun.*, vol. 3, no. 5, pp. 1802–1809, Sept. 2004.
[9] K. Lai and J. J.Shynk, "Analysis of the Linear SIC for DS/CDMA Signals with random Spreading," *IEEE Trans. Signal Processing*, vol. 52, no. 12, pp. 3417–3428, Dec. 2004.
[10] D. N. C. Tse and S. V. Hanly, "Linear Multiuser Receivers: Effective Interference, Effective Bandwidth and User Capacity," *IEEE Trans. Inform. Theory*, vol. 45, no. 2, pp. 641–657, Mar. 1999.
[11] H. Nie, P. T. Mathiopoulos, and G. K. Karagiannidis, "Reverse link capacity analysis of cellular CDMA systems with controlled power disparities and successive interference cancellation," *IEEE Trans. Wireless Commun.*, vol. 5, no. 9, pp. 2447–2457, Sept. 2006.
[12] S. Ulukus and A. Yener, "Iterative Transmitter and Receiver Optimization for CDMA Networks," *IEEE Trans. Wireless Commun.*, vol. 3, no. 6, pp. 1879–1884, Nov. 2004.
[13] A. Yener and R. D. Yates, "Multiuser access detection for CDMA systems," in *CISS'98*, pp. 17–22.
[14] D. Raychaudri, "Performance analysis of random access packet switched Code Division Multiple Access systems," *IEEE J. Select. Areas Commun.*, vol. 29, pp. 895–901, June 1981.
[15] C. Schlegel, R. Kempter, and P. Kota, "A novel random wireless packet multiple access method using CDMA," *IEEE Trans. Wireless Commun.*, vol. 5, no. 6, pp. 1362–1370, June 2006.
[16] B. Lu, X. Wang, and J. Zhang, "Throughput of CDMA data networks with multiuser detection, ARQ, and packet combining," *IEEE Trans. Wireless Commun.*, vol. 52, no. 5, pp. 811–822, May 2004.
[17] E. Malkamaki and H. Leib, "Performance of truncated type–II hybrid ARQ schemes with noisy feedback over block fading channels," *IEEE Trans. Commun.*, vol. 48, no. 9, pp. 1477–1487, Sept. 2000.
[18] Q. Zhang and S. A. Kassam, "Hybrid ARQ with selective combining for fading channel," *IEEE J. Select. Areas Commun.*, vol. 17, no. 5, pp. 867–880, May 1999.
[19] J.-F. Cheng, "Coding performance of hybrid ARQ schemes," *IEEE Trans. Commun.*, vol. 54, no. 6, pp. 1017–1029, June 2006.
[20] E. Visotsky, Y. Sun, V. Tripathi, M. L. Honig, and R. Peterson, "Reliability–based incremental redundancy with convolutional codes," *IEEE Trans. Commun.*, vol. 53, no. 6, pp. 987–997, June 2005.
[21] Q. Zhang, T. F. Wong, and S. Lehnert, "Performance of a type–II hybrid ARQ protocol in slotted DS–SSMA packet radio systems," *IEEE Trans. Commun.*, vol. 47, no. 2, pp. 281–290, Feb. 1999.
[22] R. Liu, P. Spasojevic, and E. Soljanin, "Reliable channel regions for good binary codes transmitted over parallel channels," *IEEE Trans. Inform. Theory*, vol. 52, no. 4, pp. 1405–1424, Apr. 2006.
[23] S. Sesia, G. Caire, and G. Vivier, "Incremental redundancy hybrid ARQ schemes based on low–density parity–check codes," *IEEE Trans. Commun.*, vol. 52, no. 8, pp. 1311–1321, Aug. 2004.
[24] S. Karlin and H. M. Taylor, *An introduction to stochastic modeling*. San Diego: Academic Press, 1998.
[25] Kiran and D. N. C. Tse, "Effective bandwidth and effective interference for linear multiuser receivers in asynchronous channels," *IEEE Trans. Inform. Theory*, vol. 46, no. 4, pp. 1426–1447, July 2000.
[26] L. K. Rasmussen, T. J. Lim, and A.-L. Johansson, "A matrix–algebraic approach to successive interference cancellation in CDMA," *IEEE Trans. Commun.*, vol. 48, no. 1, pp. 145–151, Jan. 2000.

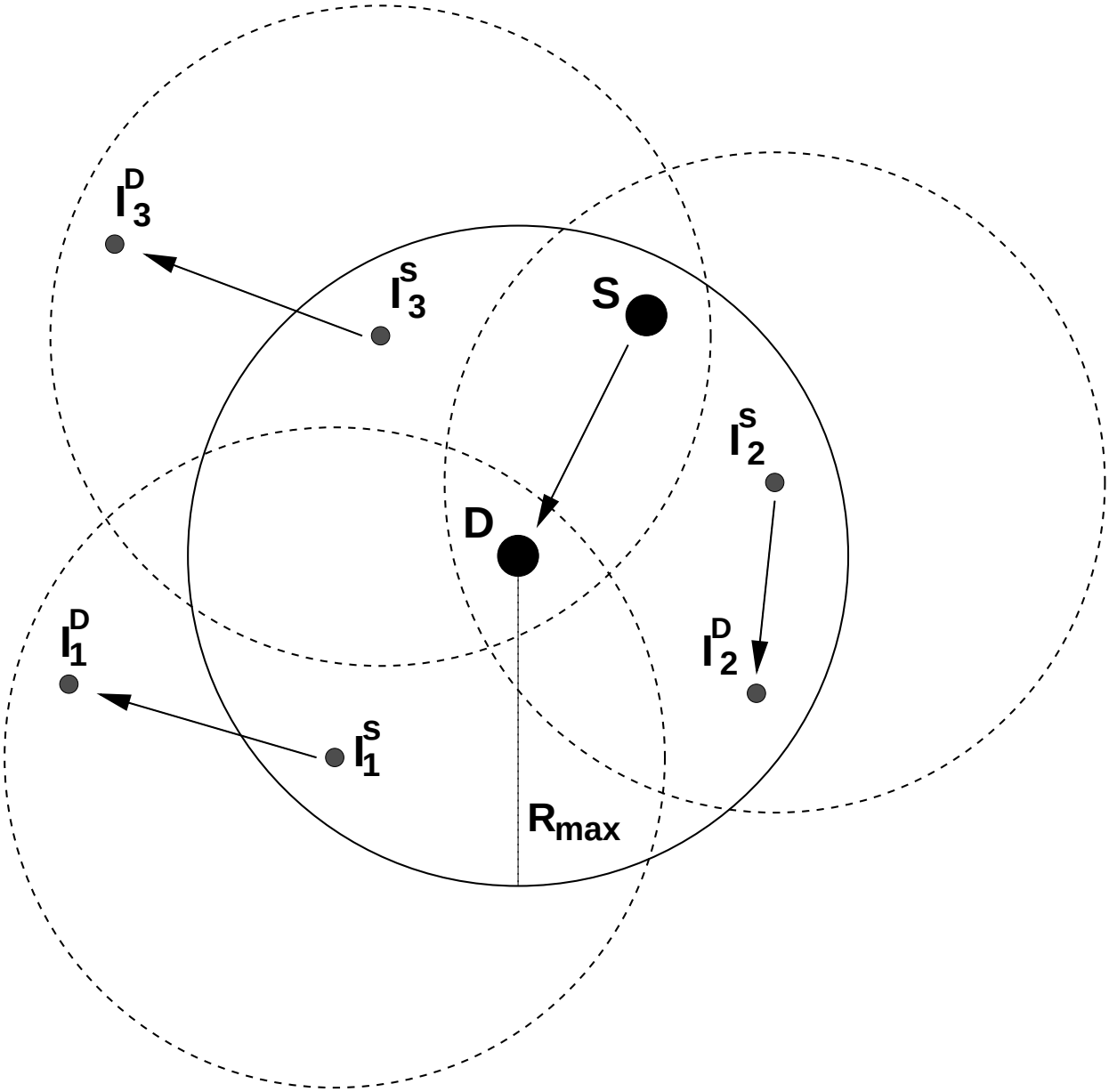

Fig. 1. Example of the considered scenario, the source and the destination are denoted with **S** and **D**, respectively. Interfering source-destination pairs are denoted with $\mathbf{I}_k^S$ and $\mathbf{I}_k^D$

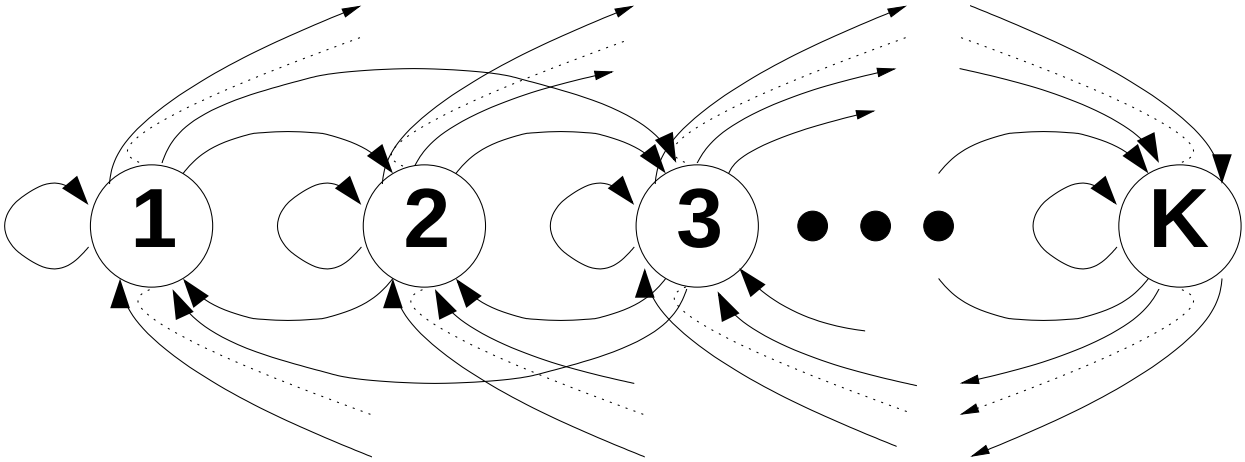

Fig. 2. Graphical representation of the embedded chain of the Semi–Markov process.

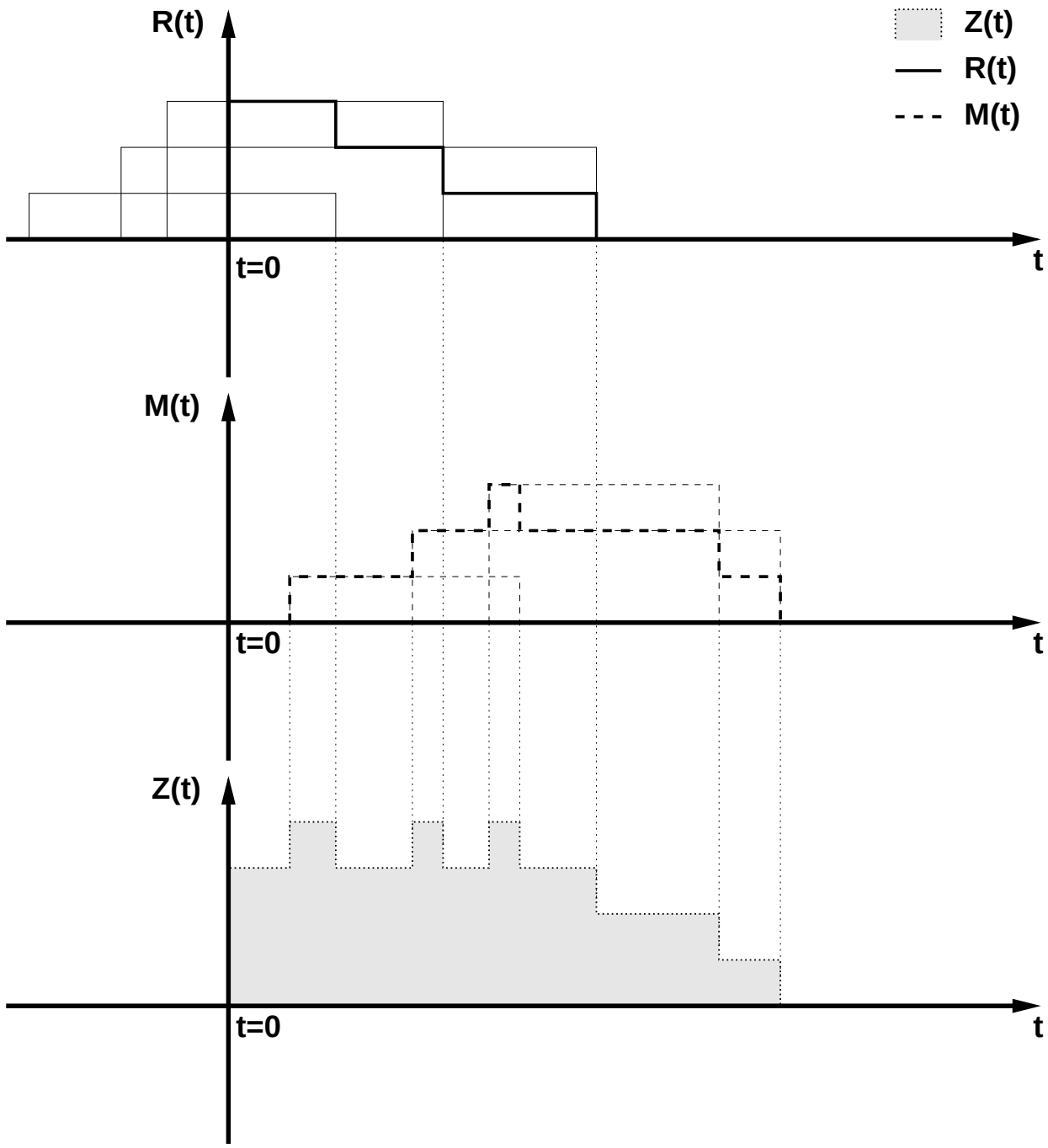

Fig. 3. Graphical representation of the arrival and departure process during a transmission. The processes that count the number of total, ongoing and new transmissions are denoted with dotted filled–gray, solid and dashed line, respectively.

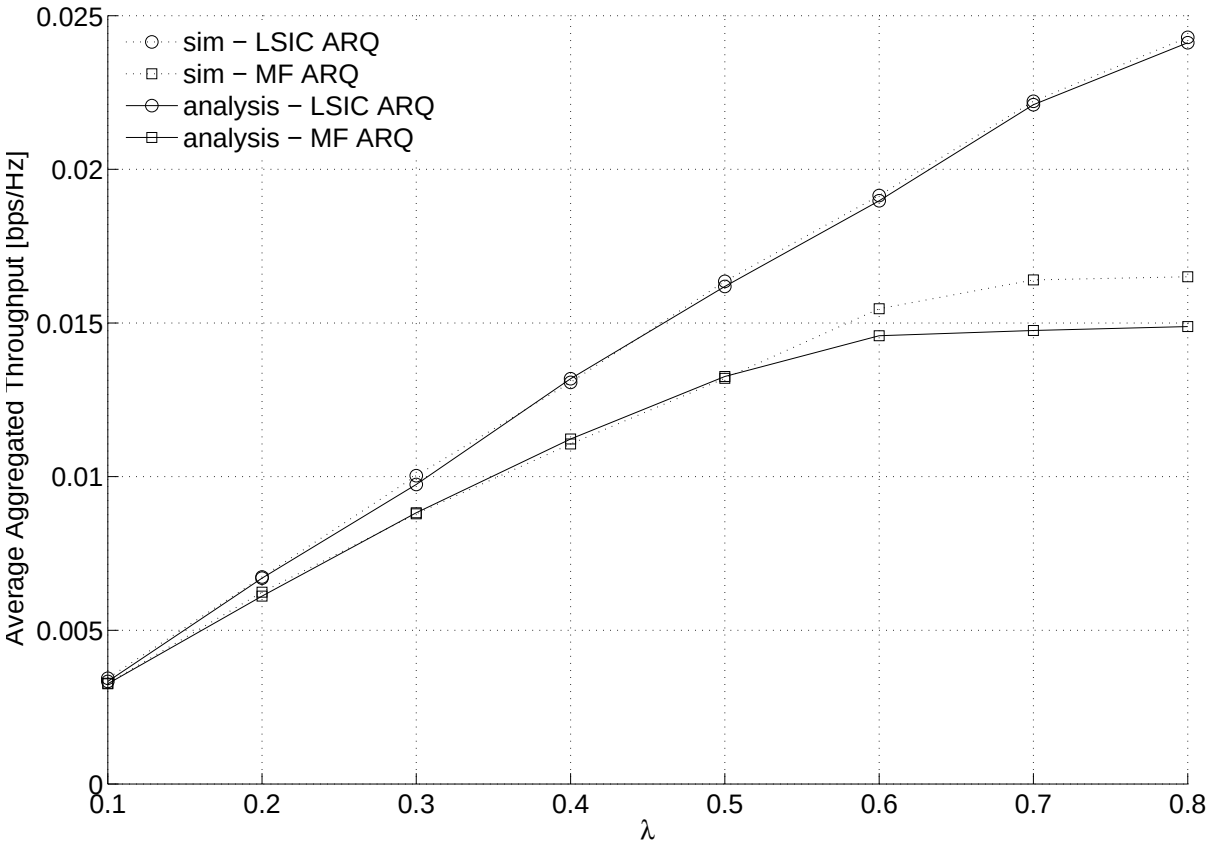

Fig. 4. Average throughput as a function of λ for the MF and MF LSIC cases, ARQ scheme, $F = 2$.

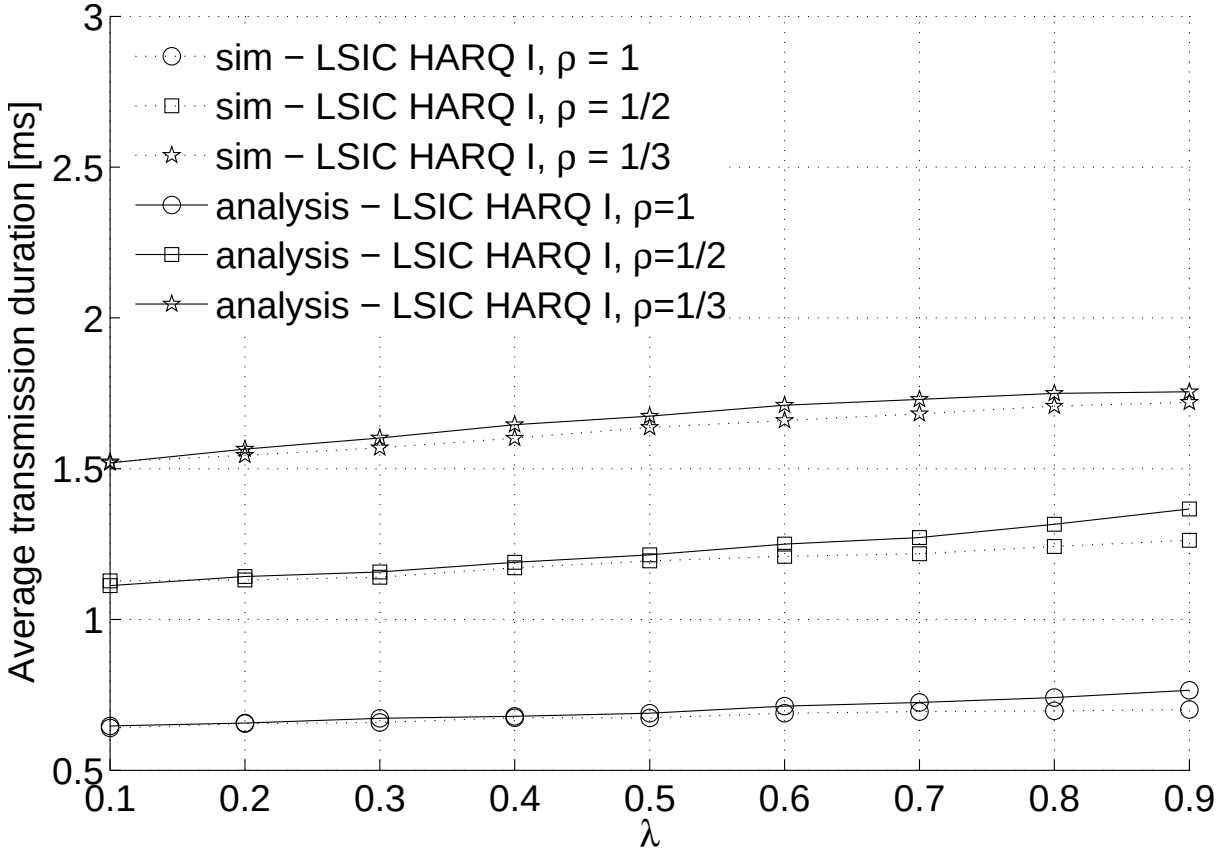

Fig. 5. Average transmission duration as a function of λ, type I HARQ scheme, $F = 2$.

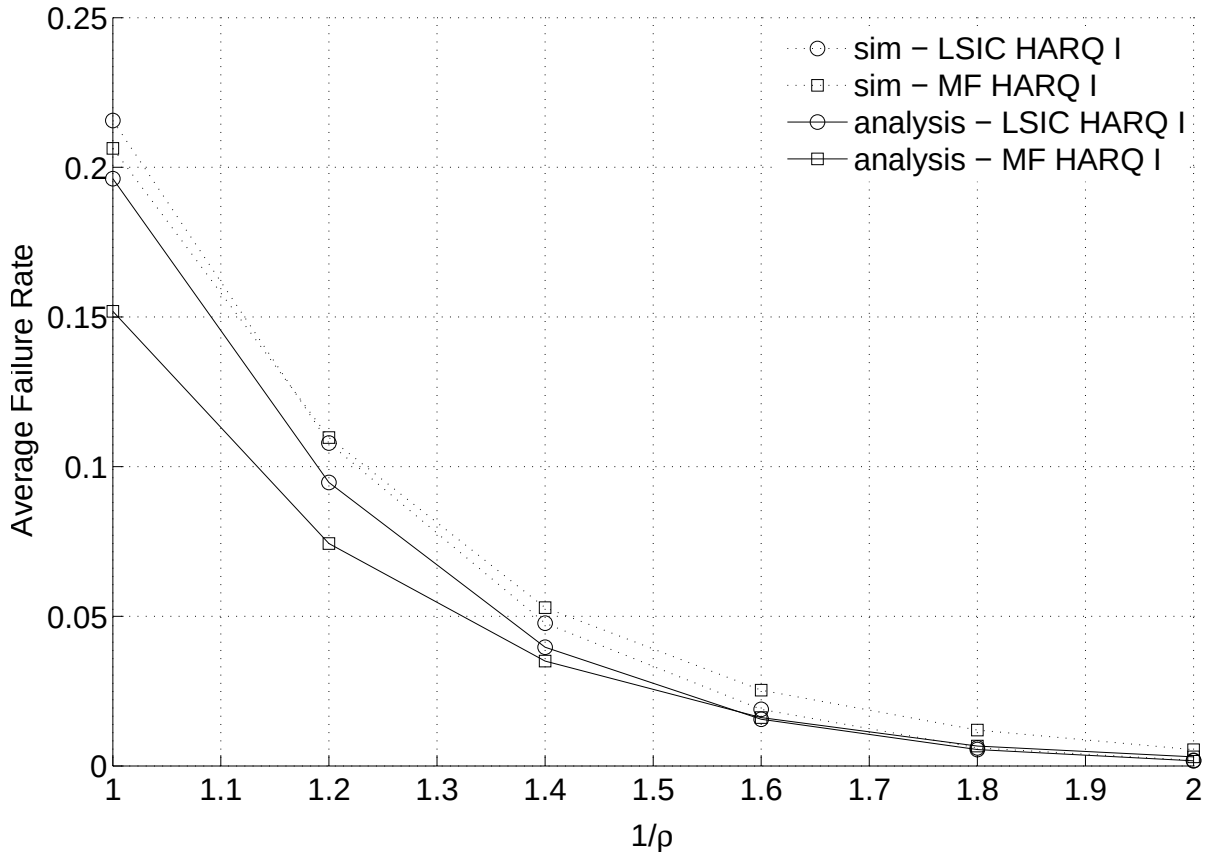

Fig. 6. Average failure probability as a function of $1/\rho$ for the MF and MF LSIC cases, type I HARQ scheme, $F = 2$, $\lambda = 0.4$.

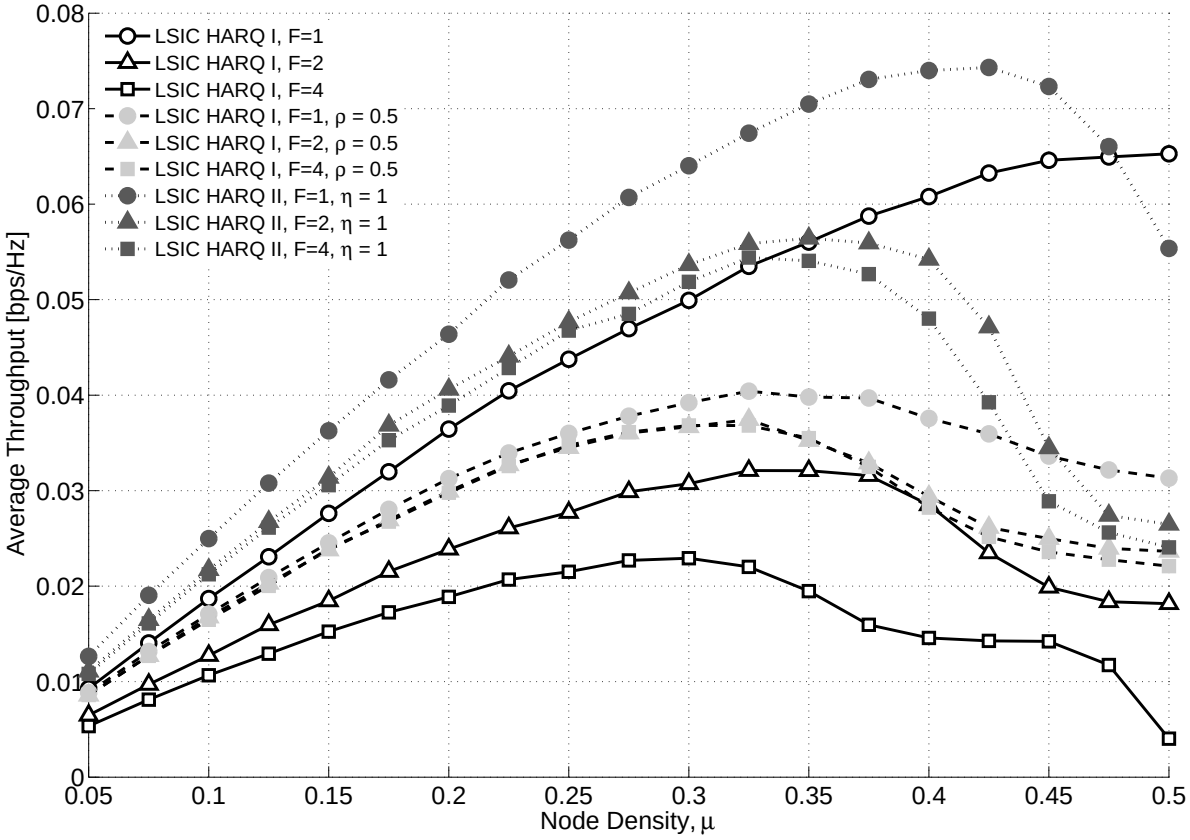

Fig. 7. Average throughput $\mathcal{R}$ as a function of the node density μ and the various proposed schemes for the MF LSIC case.

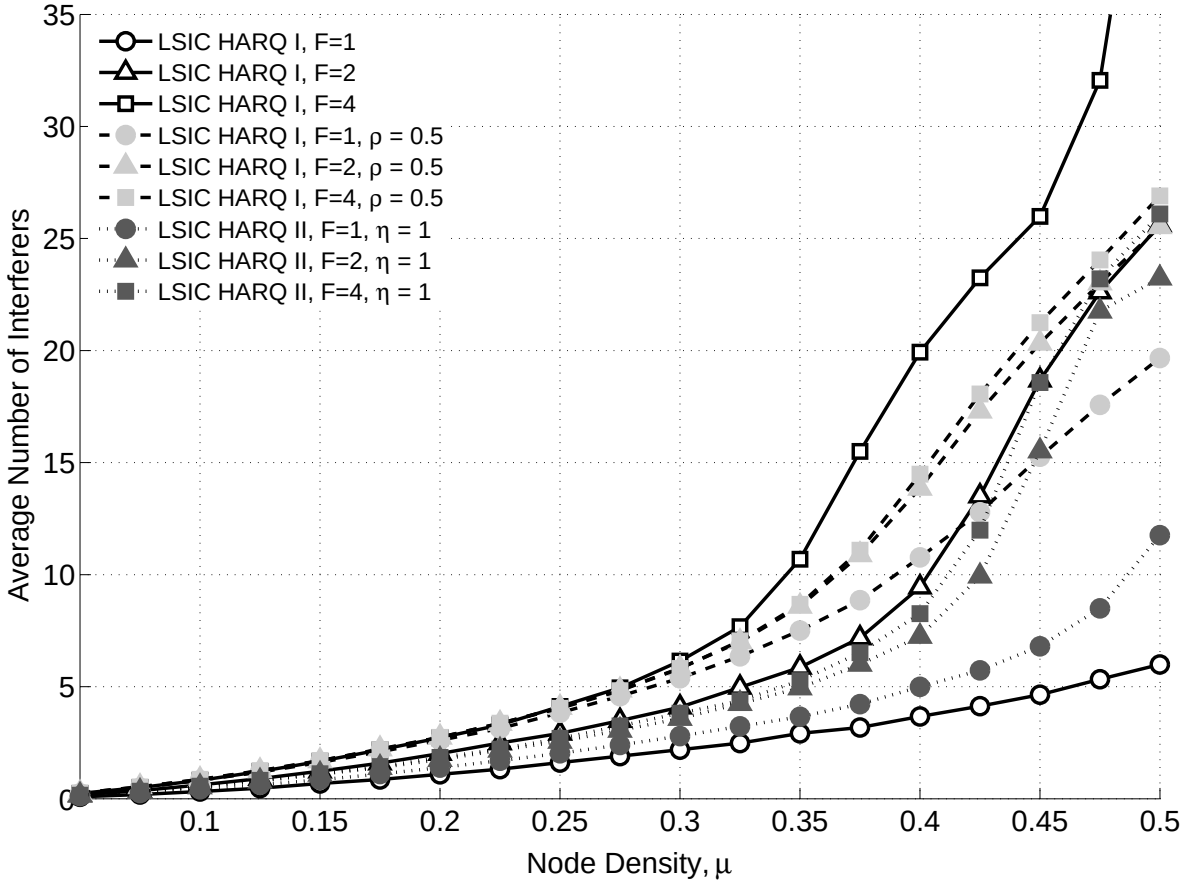

Fig. 8. Average number of interfering nodes $\mathcal{U}$ as a function of the node density μ and the various proposed schemes for the MF LSIC case.

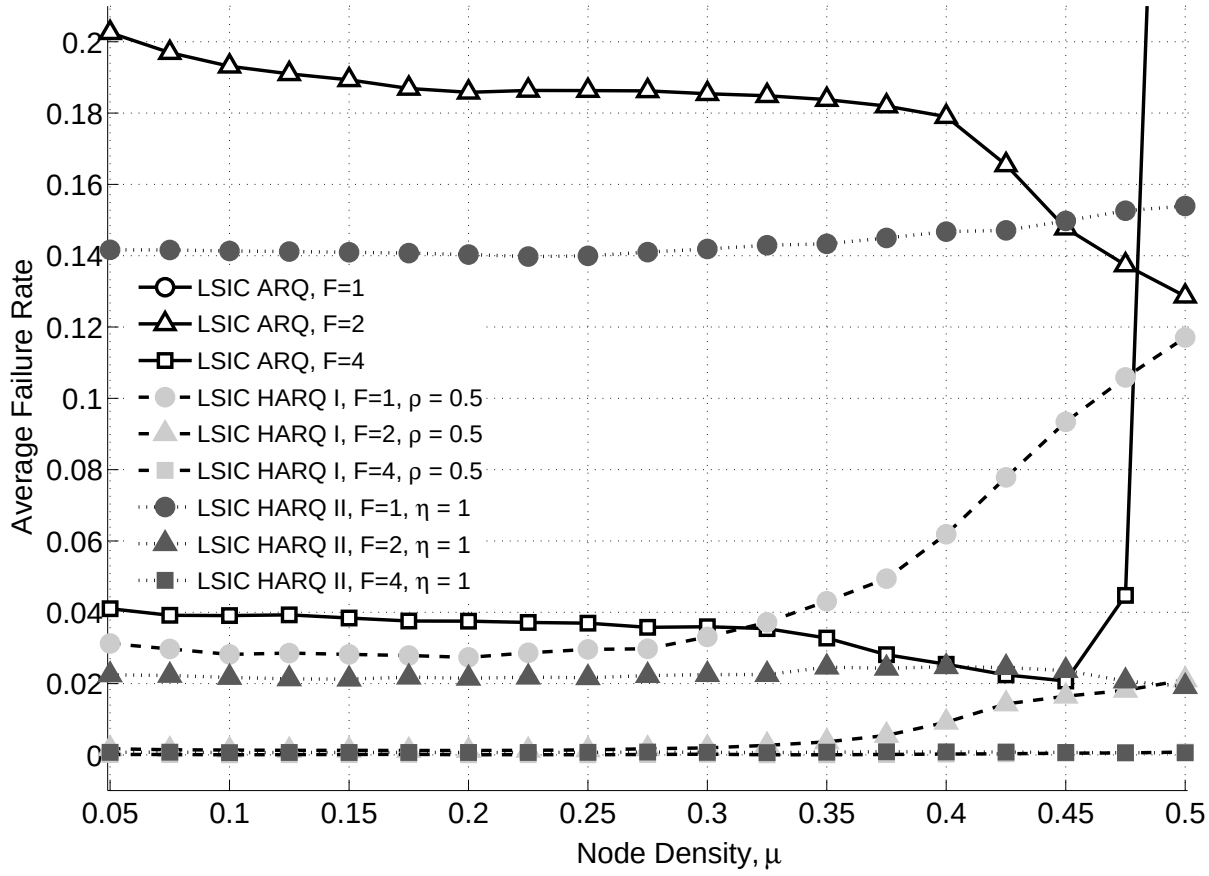

Fig. 9. Average communication failure rate Γ as a function of the node density μ and the various proposed schemes for the MF LSIC case, (the failure rate for the ARQ scheme with $F=1$ is greater than 0.4).

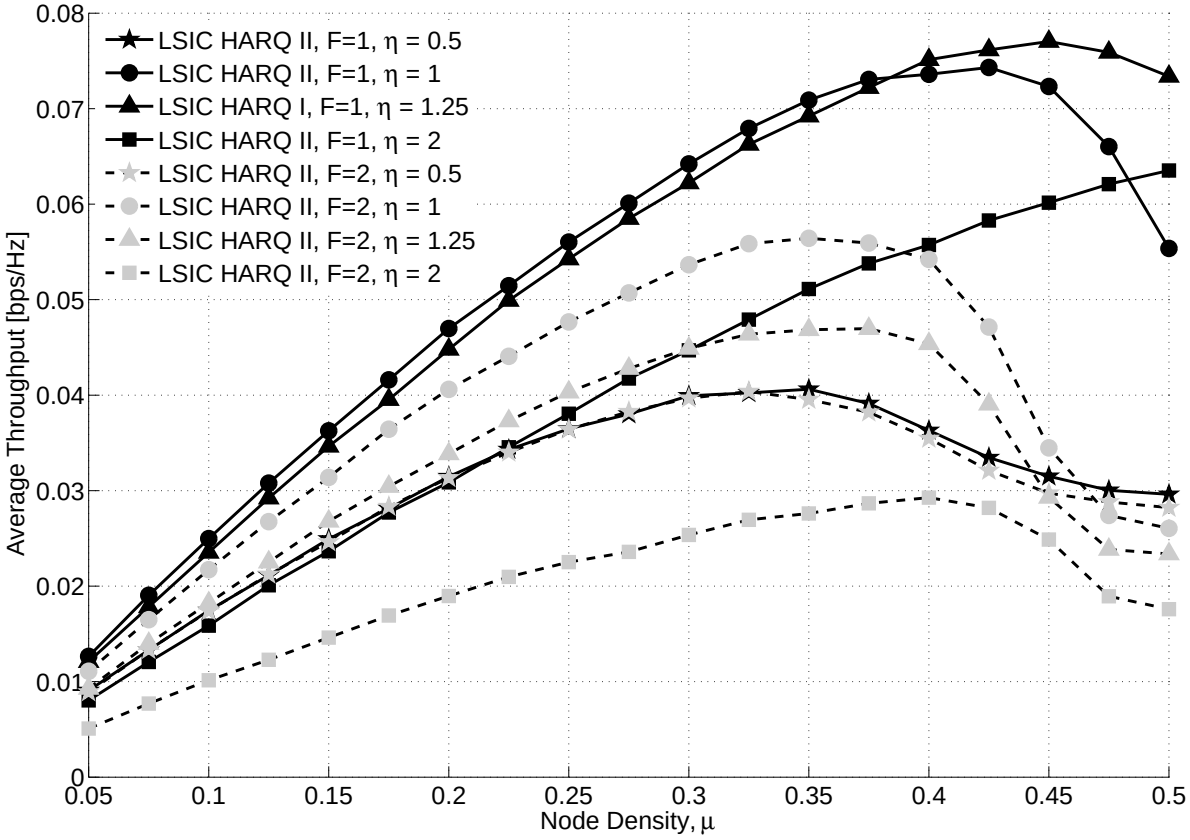

Fig. 10. Average number of interfering nodes as a function of the node density η for the type II HARQ scheme, $F = 2$.

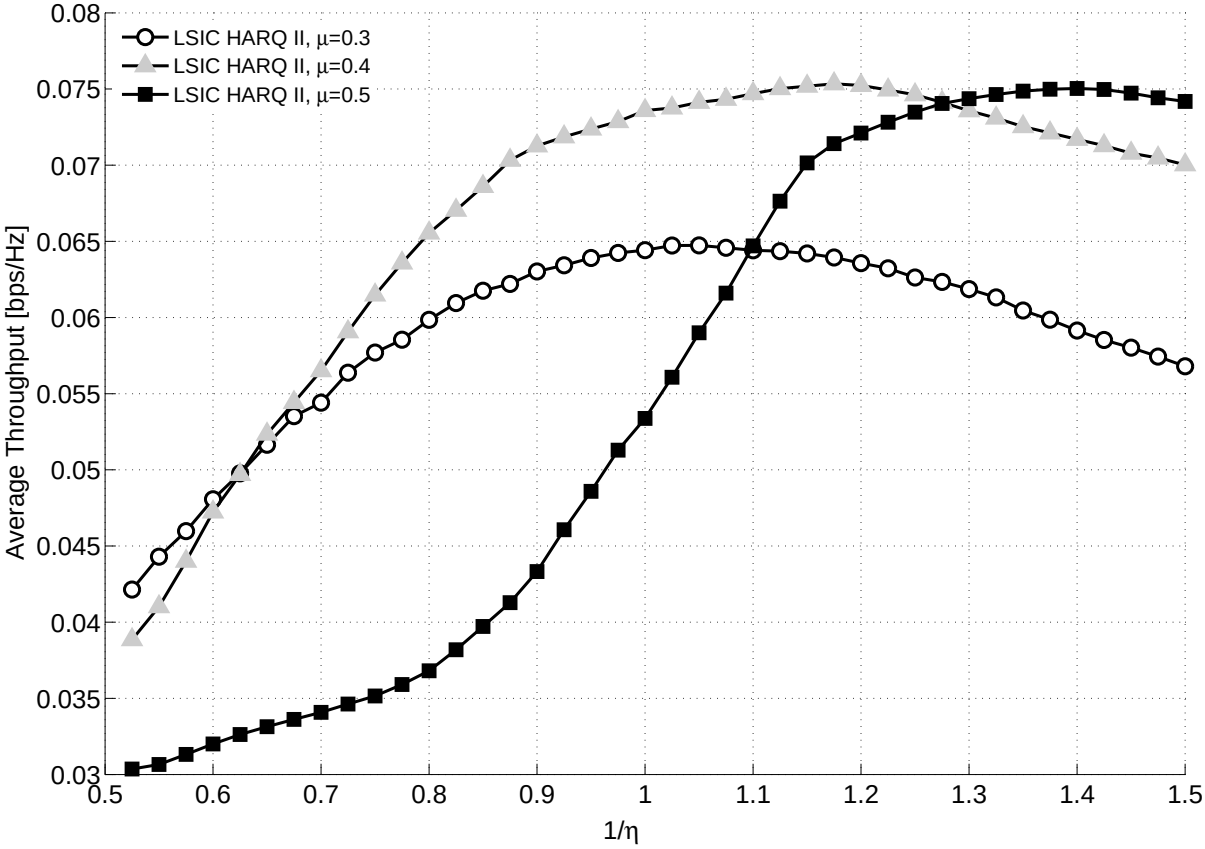

Fig. 11. Average throughput as a function of η for the type II HARQ scheme, $F = 1$.

TABLE I

TABLE OF PARAMETERS

Parameter	Value
Node density μ	0.1 nodes$/\mathrm{m}^2$
Arrival rate λ	0.4 [pkt/s]
Maximum range $R_{\max}$	100m
Available bandwidth W	$10^8/N$ Hz
Slot duration T_{S}	$2 * 10^{-5}$ s
Transmission power P_{t}/σ^2	43dB
Path loss exponent α	2
Spreading factor N	16
Uncoded packet length L	4096bits